Metric Based on Morphological Dilation for the Detection of Spatially Significant Zones

B. S. Daya Sagar, *Senior Member, IEEE*, N. Rajesh, *Member, IEEE*,
S. Ashok Vardhan, *Member, IEEE*, and Pratap Vardhan

Abstract—The ability to derive spatially significant zones (e.g., water bodies and zones of influence) within a cluster of zones has interesting applications in understanding commonly sharing physical mechanisms. Using a morphological dilation distance technique, we introduce geometric-based criteria that serve as indicator of the spatial significance of zones within a cluster of zones. This letter focuses on the problem of identifying zones that are "strategic" in the sense that they are the most central or important based on their proximity to other zones. We have applied this technique to a task aiming at detecting a spatially significant water body from a cluster of water bodies retrieved from Indian Remote Sensing Satellite Linear Imaging Self-scanning Sensor (IRS LISS-III) multispectral satellite data.

Index Terms—Dilation distance, geographic visualization, mathematical morphology, pattern classification, zones.

I. INTRODUCTION

HIGH-RESOLUTION remotely sensed satellite data and digital elevation models (DEMs) are of immense use to map spatial entities such as water bodies [1], zones of influence [2], [3], geomorphologic basins [4], [5], and urban features [6]–[14] that could be represented as areal objects on specific thematic maps. Understanding the spatial organization of such spatial entities (zones) by involving distances between all the zones of a cluster of zones is important from the point of spatial reasoning. Derivation of the spatial significance of each zone within a cluster of zones is important to decide a suitable facility (e.g., reservoir). We define a spatially significant zone as "a zone from which it is easy to reach all of its neighboring zones." A spatially significant zone should necessarily be at a strategic location and possessing a relatively larger size. A geomorphologic basin (cluster of subbasins) consists of subbasins (zones), and subbasins consist of still minor subbasins, and so on. The main geomorphologic basin that consists of subbasins is treated as a spatial system (see Fig. 1) and subbasins being subsystems. We use the terms "sets," "zones," "watersheds," "basins," and "areal objects" interchangeably in this letter.
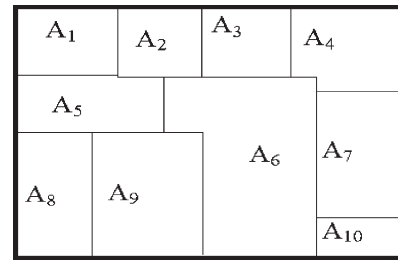
Fig. 1. Spatial system with ten zones represented over a 2-D Euclidean space. If A_i (e.g., A_1) is an origin zone, then all other zones, i.e., A_j (e.g., A_2-A_{10}), are treated as destination zones. Then, computing the degree of the spatial significance of A_i is subjected in this letter.

A spatially significant zone within a cluster of zones possesses a geometric characteristic, that is, greater proximity to other zones highlighting significance of location. Identifying the spatial significance of a zone from a geometric point of view based on qualitative spatial reasoning is nontrivial, when a spatial system includes a large number of zones, and such an identification process varies from person to person according to their own individual spatial perceptions. Recognizing spatially significant zones within such a spatial system composed of various zones could be quantitatively accomplished. In order to do so, one needs to define an appropriate measure of the spatial significance of a zone. Our concept of the spatial significance of a zone stresses on the property of a zone being central with respect to distance spatial relationship with other zones in the cluster. We maintain that, in a cluster of adjacent, nonempty compact, and nonoverlapping zones, it is possible to compare spatial significance on the basis of dilation distances. This includes the degree of proximity to other sets with minimum expenditure of energy.

The organization of this letter that attempts to provide geometric criteria to identify spatially significant zones within a cluster of zones is as follows: Section II provides modeling concepts, rationale, and methodology. Section III describes the application of the technique, whereas Section IV provides concluding observations and remarks.

II. METHODOLOGY

The goal of this section is to provide an equation based on dilation distances among zones of a cluster to automatically compute the spatial significance index (SSI) for each zone of a cluster of zones. A spatial region is a connected homogeneous 2-D cell. Its formal definition is based on point-set topology

with open and closed sets. Zones referred to in this letter are defined as subsets of a metric space such as a Euclidean space.

A. Morphological Dilation

Binary dilation is a fundamental morphological operation [15] that can be performed on any set (or map in a binary form) on a 2-D Euclidean space. We explain this transformation and its multiscale versions. The Boolean OR transformation of set A by set B is also called the dilation of A by B. The following operation in (1) dilates input image objects:

$$A \oplus B = \{a : B_a \cap A \neq \varnothing\} = \bigcup_{b \in B} A_b \qquad (1)$$

where $\oplus$ is a symbol for the morphologic dilation, $A_b = \{a + b : a \in A\}$ is the *translation* of A along vector b, and $\hat{B} = \{a : -a \in B\}$ is the symmetric of B with respect to the origin. The reader is requested to refer to [15] for a more detailed exposition of this fundamental transformation together with its algebraic properties. We shall hereafter denote the dilation of A by B by $(A \oplus B)$. Multiscale dilation can be performed by varying the size of *structuring element* nB, where $n = 0, 1, 2, \ldots, N$. Dilation can be also iteratively performed as follows:

$$(A \oplus nB) = (A \oplus B) \oplus B \oplus \cdots \oplus B. \qquad (2)$$

B. Spatial System and Its Subsystems

Let a cluster of zones, i.e., A, be composed of a number of nonempty compact sets (zones) denoted by $A_1, A_2, A_3, \ldots, A_N$ such that $A = \bigcup_{i=1}^{N} A_i$. These sets are like possible partitions of an image. A better analogy is that a DEM is an image, and possible partitions of a DEM are subbasins (zones). For any pair of zones, i.e., A_i and A_j, from this cluster, such that $i \neq j$, the following spatial relations hold true: 1) $A_i \cap (\bigcup_{\substack{j=1 \\ j \neq i}}^{N} A_j) = \varnothing$, and 2) $(A_i \oplus B) \cap (\bigcup_{\substack{j=1 \\ j \neq i}}^{N} A_j) = (((\bigcup_{\substack{j=1 \\ j \neq i}}^{N} A_j) \oplus B) \cap A_i) \neq \varnothing$.

For instance, for the cases of water bodies, nodes, and point-specific data (noncontiguous form), relation (1) would be satisfied. In many cases, where the zones are in noncontiguous form, relation (2) may not be satisfied. Relation (2) would be satisfied if all the zones of a cluster are in a contiguous form (e.g., zones of influence of water bodies). In this letter, we consider both cases that respectively satisfy relations (1) and (2).

C. Dilation Distances Between Origin and Destination Zones

Determining distances between spatial objects (zones) based on Euclidean metric is a challenge. If all the zones in a cluster considered are identical such that the shapes and sizes of zones are similar, then the simple Euclidean distances between all the possible pairs of centroids of such zones would suffice to detect the spatially significant centroid corresponding to a zone. Euclidean distance of centroids of zones possessing dissimilar shapes and sizes would lead to a problem in detecting the precise spatially significant zone due to the following reasons: 1) Computation of centroids of zones requires an additional step
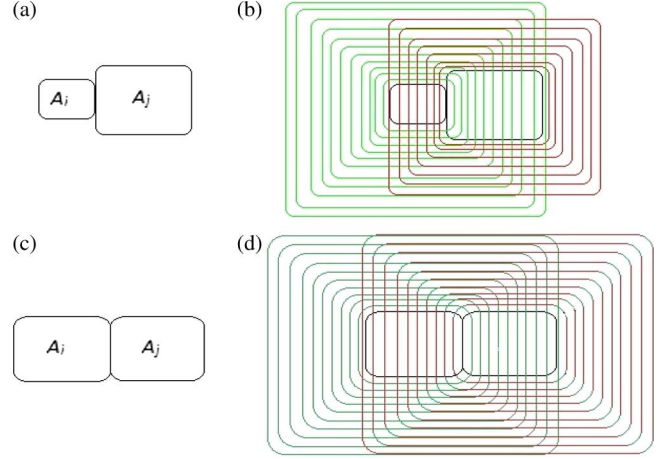

Fig. 2. (a) Two homothetic adjacent sets A_i and A_j of different sizes. (b) Dilation distances $d(A_{ij}) = 11$ and $d(A_{ji}) = 7$ and, in turn, $\rho(A_{ij}) = 7$. (c) Two geometrically similar homothetic adjacent sets A_i and A_j of similar sizes. (d) Dilation distances $d(A_{ij}) = 10$ and $d(A_{ji}) = 10$ and, in turn, $\rho(A_{ij}) = 10$.

perhaps based on a "minimal skeletal point" that is computationally expensive, and 2) the Euclidean distance between the centroids of the two zones does not explain the morphological (geometric) properties of the zones under consideration. However, the iterative dilation is a better choice to compute distances between zones. Dilation distance is employed to address the topic of identifying the spatially significant zone(s) from a cluster of zones of varied shapes and sizes.

Let nonempty disjoint compact zones A_i and A_j be the origin and destination zones, respectively. A_i is smaller than A_j [see Fig. 2(a)]. The dilation distance from A_i to A_j [see Fig. 2(b)] is represented by

$$d(A_{ij}) = \min_{i \neq j} (n : A_j \subseteq (A_i \oplus nB)). \qquad (3)$$

Similarly, the dilation distance from A_j to A_i is represented by

$$d(A_{ji}) = \min_{i \neq j} (n : A_i \subseteq (A_j \oplus nB)). \qquad (4)$$

We may state the following: $d(A_{ii}) = 0$, $d(A_{ij}) \neq d(A_{ji})$, and $d(A_{ij}) = d(A_{ji})$ if both A_i and A_j possess identical size, shape, and orientation [see Fig. 2(c) and (d)]. From (3) and (4), it is evident that a smaller object, to completely occupy a relatively larger one, requires a greater number of dilation cycles than in the converse scenario [see Fig. 2(a) and (b)]. If there exists a shape–size dissimilarity between the two sets, one can observe that $d(A_{ij}) \neq d(A_{ji})$, and the minimum of $d(A_{ij})$ and $d(A_{ji})$ is the Hausdorff dilation distance in (5) [16], [17], i.e.,

$$\rho(A_{ij}) = \min (d : d(A_{ij}), d(A_{ji})). \qquad (5)$$

Estimation of the dilation distance between the origin and destination zones is justified, as such a dilation distance is essential to compute distances between the zones. The limitation of this distance is that it is essentially affected by the object's

boundary points that are farthest out with respect to other spatial objects.

The maximum distance $d_{\max}$ between an origin zone A_i and destination zones A_j of a cluster is computed as

$$d_{\max}(A_{ij}) = \max_{\forall j} \left(\min \left(n : \left(A_j \subseteq (A_i \oplus nB) \right) \right) \right)$$

$$= \min \left\{ n : \left(\bigcup_{\substack{j=1 \\ j \neq i}}^{N} A_j \right) \subseteq (A_i \oplus nB) \right\}. \quad (6)$$

Similarly, $d_{\max}$ between the destination zones and an origin zone is computed as

$$d_{\max}(A_{ji}) = \max_{\forall j} \left(\min \left(n : \left(A_i \subseteq (A_j \oplus nB) \right) \right) \right). \quad (7)$$

The maximum over all the distances between A_i and A_j in (6) and (7) explains how many minimum dilation cycles are required to cover the union of all A_js.

D. SSI of a Zone

A zone A_i is designated as spatially most significant to establish a facility if it is located in a place closer to all A_js and reaching A_i from all A_js required a shorter distance (minimum energy expenditure involved). No other zone from a cluster of A_js matches with A_i with respect to these two characteristic (spatial) relationships, and hence, A_i is chosen as the best zone and is termed as the most spatially important zone. Keeping these characteristics in view, we propose (8) involving dilation distances between origin zone A_i and destination zones A_j. Thus

$$\text{SSI} = \min_{\forall i} \left(d_{\max}(A_{ij}) \right). \quad (8)$$

The minimum of all the maximum values of the corresponding origin zones would explain about the zone from which it is easier to reach out all other zones with minimum energy expenditure (dilation distance). The SSI of zone A_i is a dimensionless unit. The lower the SSI of zone A_i in a cluster of zones, the higher is its significance. Equation (9) that computes the normalized spatial significance index (NSSI) that ranges between 0 and 1 takes the form

$$\text{NSSI} = \left(\frac{\min\limits_{\forall i} \left(d_{\max}(A_{ij}) \right)}{\max\limits_{\forall i} \left(d_{\max}(A_{ij}) \right)} \right). \quad (9)$$

A low value of the SSI or the NSSI enables the location significance/importance of zone A_i from which every other zone could be reached, or zone A_i could be reached from every other zone with minimum expenditure of energy. If the zones of a cluster are not similar in shape and/or size, then $\min_{\forall i}(d_{\max}(A_{ij}))$ and $\min_{\forall j}(d_{\max}(A_{ji}))$ are not equal. They are equal if the shapes and sizes of zones of a cluster are identical to each other. When all zones in a cluster are similar both in terms of size and shape, the following relationship holds good:

$$\left(\frac{\min\limits_{\forall i} \left(d_{\max}(A_{ij}) \right)}{\max\limits_{\forall i} \left(d_{\max}(A_{ij}) \right)} \right) = \left(\frac{\min\limits_{\forall j} \left(d_{\max}(A_{ji}) \right)}{\max\limits_{\forall j} \left(d_{\max}(A_{ji}) \right)} \right). \quad (10)$$
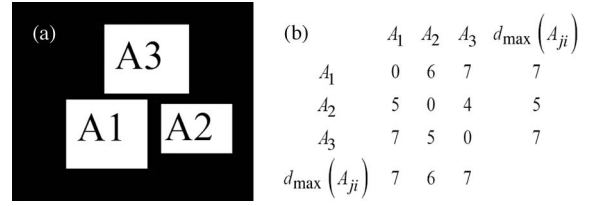

Fig. 3. (a) Synthetic example consisting of three spatial objects. (b) Dilation distances between every possible pair are shown in a matrix form in addition to the values obtained according to (6) and (7).

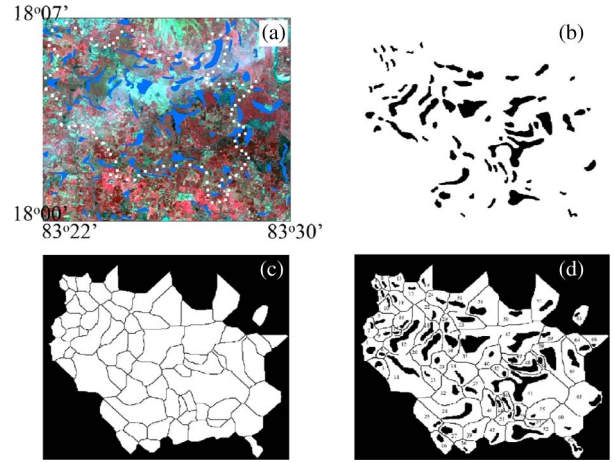|	A_1	A_2	A_3	$d_{\max}\left(A_{ji}\right)$
A_1	0	6	7	7
A_2	5	0	4	5
A_3	7	5	0	7
$d_{\max}\left(A_{ji}\right)$	7	6	7	

Fig. 4. (a) Indian Remote Sensing satellite (IRS LISS-III) multispectral image of the study area. The blue objects are water bodies traced from the IRS LISS-III image with the topographic map reference superposed on the IRS LISS-III image, and white dots indicate the boundary of the considered cluster. (b) Small water bodies. (c) Zones of influence of corresponding water bodies. (d) Water bodies and zones of influence with labeling.

This relationship also holds good for cases where centroids of zones are considered. The synthetic example that follows may be referred for more details.

E. Synthetic Example

For clarity, a synthetic example is given to explain (6)–(10). Let A_1, A_2, and A_3 be three spatial objects in a cluster [see Fig. 3(a)]. The assumed distances between all possible pairs of these three spatial objects are shown in Fig. 3(b). A corresponding matrix is shown in Fig. 3(b) from which $d_{\max}(A_{ij})$, $d_{\max}(A_{ji})$, the SSI, the NSSI, and the homogeneity degree of spatial objects explained in (6)–(10) could be easily understood.

As per the SSI and the NSSI (i.e., 6 and 0.857) computed according to (8) and (9), respectively, where the considered data include assumed dilation distances [see Fig. 3(b)], A_2 is designated as the spatially significant zone.

III. EXPERIMENTAL RESULTS

A. Cluster of Zones of Water Body Influence

Small water bodies and their zones of influence of varied sizes and shapes heterogeneously arranged [see Fig. 4(a)–(d)] are good examples of spatial systems. The data, which are sourced from IRS LISS-III multispectral data of 23.5 mts spatial resolution [see Fig. 4(a)] and a topographic map of
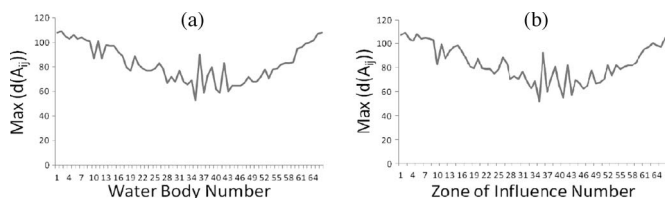
Fig. 5. (a) Max($d(A_{ij})$) for all *is*. (b) Max($d(Z_{ij})$).

TABLE I
SSIs of Top Five Water Bodies and Zones

Rank	Water Body (W) Label	D-Dist	Zone (Z) Label	D-Dist	NSSI (W)	NSSI (Z)
1	35	53	35	52	0.48	0.47
2	41	59	41	55	0.54	0.50
3	43	59	43	57	0.54	0.51
4	49	60	37	60	0.55	0.54
5	46	62	46	62	0.56	0.56

a region situated in between the geographical coordinates $18°00'-18°07'$N and $83°22'-83°30'$E, have been employed. Sixty-six water bodies were traced from IRS LISS-III multi-spectral data with the topographic map reference [see Fig. 4(b)]. The corresponding 66 influence zones, which are defined as the catchment basins of the corresponding water bodies (markers), computed by using the technique of *skeletonization by zones of influence* are shown in Fig. 4(c). Since the region considered is in slope category of $< 2°$ slope, the elevation differences across the region considered are minimal, and hence, the region is treated as flat. In view of this fact, a DEM has not been used. Water bodies and zones respectively representing markers and catchment basins are denoted by A_i with proper labeling [see Fig. 4(d)]. Dilation distances, which are essential parameters of (8) and (9), between each water body (zone) and all other destination water bodies (zones) in a cluster of water bodies (zones) are respectively computed according to (3) and (4) and are shown in a supporting nonprint material, along with an adjacency matrix of dimensions 66×66, representing zones adjacent to each zone.

Maximum dilation distances observed from the distances computed between every water body and every other water body belonging to a cluster of 66 water bodies are plotted as functions of water bodies [see Fig. 5(a)]. Similar maximum dilation distances observed from the estimated distances between every zone of influence to every other zone of influence are also plotted as functions of zones of influence [see Fig. 5(b)]. The observed minimum distances among 66 maximum distances for both water bodies [see Fig. 5(a)] and zones [see Fig. 5(b)] include 53 and 52, respectively (see Table I). This table also provides details of other four spatially significant water bodies and zones of influence. The maximum distances among 66 maximum distances for both water bodies and zones observed include 109 and 110, respectively.

As per (8) and (9), we found out that the water body labeled as 35 and the zone labeled as 35 are spatially significant. The corresponding water body and zone of influence are shown in Fig. 6(a) and (b), respectively. SSIs of 66 water bodies and 66 zones of water body influence are shown. The lower the
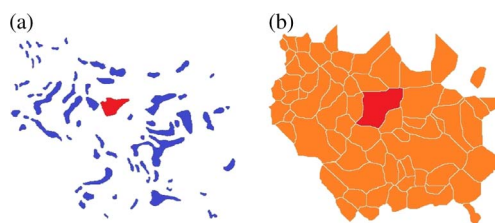

Fig. 6. Spatially significant (a) water body labeled as 35 (red color) and (b) zone of water body influence labeled as 35 (red color).
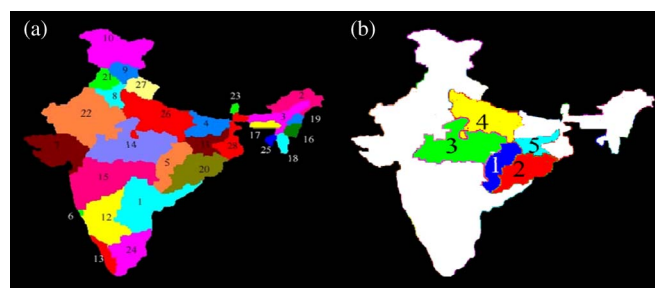

Fig. 7. (a) Map of India (spatial system) with 28 states (zones), indexed according to alphabetical order: Andhra Pradesh (A_1), Arunachal Pradesh (A_2), Assam (A_3), Bihar (A_4), Chhattisgarh (A_5), Goa (A_6), Gujarat (A_7), Haryana (A_8), Himachal Pradesh (A_9), Jammu and Kashmir (A_{10}), Jarkhand (A_{11}), Karnataka (A_{12}), Kerala (A_{13}), Madhya Pradesh (A_{14}), Maharashtra (A_{15}), Manipur (A_{16}), Meghalaya (A_{17}), Mizoram (A_{18}), Nagaland (A_{19}), Orissa (A_{20}), Punjab (A_{21}), Rajasthan (A_{22}), Sikkim (A_{23}), Tamilnadu (A_{24}), Tripura (A_{25}), Uttarapradesh (A_{26}), Uttarakhand (A_{27}), West Bengal (A_{28}). (b) First five spatially significant states with their ranks.

index, the higher is the spatial significance. The zones labeled as 35, 41, 43, 37, and 46 are the five best zones that have SSIs of 52, 55, 57, 60, and 62, respectively. The corresponding NSSIs for these zones include 0.47, 0.50, 0.51, 0.54, and 0.56, respectively. The SSIs and NSSIs for water bodies are also shown in Table I. Interestingly, these spatially significant water body [see Fig. 6(a)] and zone of influence [see Fig. 6(b)] possess longer boundary being shared with neighboring water bodies/zones of influence.

B. States of India

The approach demonstrated on a cluster of water bodies has been extended to recognize a spatially significant state from a cluster of 28 states of India [see Fig. 7(a)]. The dilation distances between every state to every other state are estimated, and origin-state specific maximum distances are computed (supporting material). Maximum dilation distances observed from the estimated distances between every state and every other state of a cluster of 28 states of India are considered, and the minimum of these maximum distances is considered to detect the spatially significant state. The minimum of all these maximum distances is 189, which is followed by 206, 213, 226, and 233. The maximum of maximum distances estimated between each origin state and all destination states is 383. The NSSI is computed according to (9). The first five states that possess the minimum of maximum distances are shown in Fig. 7(b), and their corresponding SSIs and NSSIs are shown in Table II.

TABLE II
SSIs OF TOP FIVE STATES

RANK	STATE LABEL	D-DIST	NSSI
1	5	189	0.49
2	20	206	0.53
3	14	213	0.55
4	26	226	0.59
5	11	233	0.60

On Intel Core 2 Duo T5850 at 2.17 GHz with 3-GB random access memory on a 32-bit operating system, it took 30, 31, and 17 min, respectively, to compute the dilation distances for the following cases: 1) 66 water bodies (400×400 pixels); 2) 66 zones of influence (400×400 pixels); and 3) 28 states of India (480×480 pixels). The number of dilation distances required to be computed increases with the number of spatial objects and the sizes of the individual spatial objects. Hence, the computational complexity increases with increasing number of spatial objects and spatial resolution. This time could be significantly reduced by rescaling the data such that the zones of the cluster do not lose their shape characteristics.

IV. CONCLUSION

The technique proposed here provided the SSI for zones of a cluster of zones. Identifying a spatially significant zone via (8) is a scale-invariant process. This equation is sensitive to variations in rotations and translations and to geometric distortions but insensitive to variations in the scale of the considered zones. Mostly, a larger interior zone that could be reached by other destination zones of a cluster would stand as a spatially significant zone. Although the application of this technique is shown for data represented in raster format, without significant computational difficulty, this technique can be extended to: 1) a wide class of metric spaces and to other representations (such as objects bounded by 2-D vectors); and 2) a 3-D case, i.e., by replacing the dilation distance with gray-scale geodesic distances. This approach provides useful insights in the following: 1) clustering–classification frameworks; 2) detecting the spatially significant segmented zones (spatial objects in a 2-D case) obtained via various segmentation approaches; 3) automatically deriving a central node from a large number of nodes; 4) determining the influence of a node in a vector-based network setting; and 5) deciding on nodal center(s) to establish an administrative facility from a cluster of cadastral zones mapped from remotely sensed satellite data.

REFERENCES

[1] B. S. D. Sagar, G. Gandhi, and B. S. P. Rao, "Applications of mathematical morphology on water body studies," *Int. J. Remote Sens.*, vol. 16, no. 8, pp. 1495–1502, 1995.

[2] B. S. D. Sagar, "Universal scaling laws in surface water bodies and their zones of influence," *Water Resour. Res.*, vol. 43, no. 2, pp. W02416-1–W02416-10, 2007.

[3] H. M. Rajashekara, P. Vardhan, and B. S. D. Sagar, "Generation of zonal map from point data via weighted skeletonization by influence zone," *IEEE Geosci. Remote Sens. Lett.*, vol. 9, no. 3, pp. 403–407, May 2012.

[4] L. T. Tay, B. S. D. Sagar, and H. T. Chuah, "Analysis of geophysical networks derived from multiscale digital elevation models: A morphological approach," *IEEE Geosci. Remote Sens. Lett.*, vol. 2, no. 4, pp. 399–403, Oct. 2005.

[5] L. T. Tay, B. S. D. Sagar, and H. T. Chuah, "Granulometric analysis of basin-wise DEMs: A comparative study," *Int. J. Remote Sens.*, vol. 28, no. 15, pp. 3363–3378, Jul. 2007.

[6] M. Pesaresi and J. A. Benediktsson, "A new approach for the morphological segmentation of high-resolution satellite imagery," *IEEE Trans. Geosci. Remote Sens.*, vol. 39, no. 2, pp. 309–320, Feb. 2001.

[7] J. A. Benediktsson, M. Pesaresi, and K. Arnason, "Classification and feature extraction for remote sensing images from urban areas based on morphological transformations," *IEEE Trans. Geosci. Remote Sens.*, vol. 41, no. 9, pp. 1940–1949, Sep. 2003.

[8] T. Barata and P. Pina, "A morphological approach for feature space partitioning," *IEEE Geosci. Remote Sens. Lett.*, vol. 3, no. 1, pp. 173–177, Jan. 2006.

[9] H. Taubenbock, M. Habermeyer, A. Roth, and S. Dech, "Automated allocation of highly structured urban areas in homogeneous zones from remote sensing data by Savitzky–Golay filtering and curve sketching," *IEEE Geosci. Remote Sens. Lett.*, vol. 3, no. 4, pp. 532–536, Oct. 2006.

[10] J. Chanussot, J. A. Benediktsson, and M. Fauvel, "Classification of remote sensing images from urban areas using a fuzzy possibilistic model," *IEEE Geosci. Remote Sens. Lett.*, vol. 3, no. 1, pp. 40–44, Jan. 2006.

[11] M. Dalla Mura, A. Villa, J. A. Benediktsson, J. Chanussot, and L. Bruzzone, "Classification of hyperspectral images by using extended morphological attribute profiles and independent component analysis," *IEEE Geosci. Remote Sens. Lett.*, vol. 8, no. 3, pp. 542–546, May 2011.

[12] C. Mering, J. Baro, and E. Upegui, "Retrieving urban areas on Google Earth images: Application to towns of West Africa," *Int. J. Remote Sens.*, vol. 31, no. 22, pp. 5867–5877, Nov. 2010.

[13] A. Wilson, "Remote sensing as the 'X-ray crystallography' for urban 'DNA'," *Int. J. Remote Sens.*, vol. 31, no. 22, pp. 5993–6003, Nov. 2010.

[14] G. Trianni, F. Dell'Acqua, and P. Gamba, "Geographic information system (GIS)-aided per-segment scene analysis of multi-temporal spaceborne synthetic aperture radar (SAR) series with application to urban area," *Int. J. Remote Sens.*, vol. 31, no. 22, pp. 6005–6014, Nov. 2010.

[15] J. Serra, *Image Analysis and Mathematical Morphology*. London, U.K.: Academic, 1982.

[16] J. Serra, "Hausdorff distances and interpolations," in *Mathematical Morphology and Its Applications to Images and Signal Processing*, H. J. A. M. Heijmans and J. B. T. M. Roerdink, Eds. Dordrecht, The Netherlands: Kluwer, 1998.

[17] B. S. D. Sagar, "Visualization of spatiotemporal behavior of discrete maps via generation of recursive median elements," *IEEE Trans. Pattern Anal. Mach. Intell.*, vol. 32, no. 2, pp. 378–384, Feb. 2010.